BOSE–EINSTEIN CORRELATIONS AND JET STRUCTURE OF HADRONIC Z DECAYS*

W.J. Metzger

for the L3 Collaboration

IMAPP, Radboud University, 6525 AJ Nijmegen, The Netherlands

(Received January 25, 2013)

Bose–Einstein correlations of pairs of identical charged pions produced in hadronic Z decays are analyzed for various jet configurations, varying from narrow two-jet events to well-separated three-jet events. Parametrizations suggested by the τ-model are used to fit the Bose–Einstein correlation function both as a function of the invariant four-momentum difference and of its components in the Longitudinal Center of Mass frame. The resulting values of the radii are found to depend on the jet structure of the event.

DOI:10.5506/APhysPolBSupp.6.491
PACS numbers: 13.87.Fh, 13.66.Bc

1. Introduction

We have recently published [1] a study of Bose–Einstein correlations (BEC) in hadronic Z decay where we found good agreement with parametrizations arising in the τ-model [2, 3].

In this paper, new *preliminary* results are presented for various jet configurations ranging from narrow two-jet to well-separated three-jet events.

The data were collected by the L3 detector at an e^+e^- center-of-mass energy of $\sqrt{s} \simeq 91.2$ GeV. Approximately 36 million like-sign pairs of well-measured charged tracks from about 0.8 million hadronic Z decays are used. This data sample is identical to that of Ref. [1].

Two-pion BEC are measured by $R_2(Q) = \rho(Q)/\rho_0(Q)$, where $\rho(Q)$ is the density of pairs with invariant four-momentum difference $Q = \sqrt{-(p_1 - p_2)^2}$ and $\rho_0(Q)$ is the similar density in an artificially constructed reference sample, which should differ from the data only in that it does not contain BEC. The same event mixing technique is used to construct ρ_0 as in Ref. [1].

* Presented at the International Symposium on Multiparticle Dynamics, Kielce, Poland, September 17–21, 2012.

In the τ-model, R_2 is found to depend not only on Q, but also on quantities a_1 and a_2, where for two-jet events $a = 1/m_t$ (m_t being the transverse mass of a particle). Parameters of the model are the parameters of the Lévy distribution which describes the proper time of particle emission: α, the index of stability of the Lévy distribution, a width parameter, and the proper time τ_0 at which particle production begins. We shall use a simplified parametrization [1], where τ_0 is assumed to be zero and a_1 and a_2 are combined with $\Delta\tau$ to form an effective radius R:

$$R_2(Q) = \gamma \left[1 + \lambda \cos\left((R_a Q)^{2\alpha}\right) \exp\left(-(RQ)^{2\alpha}\right)\right](1 + \epsilon Q)\,, \qquad (1)$$

where

$$R_a^{2\alpha} = \tan\left(\frac{\alpha\pi}{2}\right) R^{2\alpha}\,. \qquad (2)$$

It is perhaps surprizing that Eq. (1) agrees well with three-jet events as well as with two-jet events [1], since the τ-model is inspired by a picture of fragmentation of a single string.

It must also be pointed out that the τ-model has its shortcomings: The τ-model predicts that R_2 depends on the two-particle momentum difference only through Q, not through components of Q. However, this is not the case [1]. Nevertheless, regardless of the validity of the τ-model, Eq. (1) provides a good description of the data. Accordingly, we shall use it in the following.

Using the Durham and JADE algorithms, events can be classified according to the number of jets. The number of jets in a particular event depends on the jet resolution parameter of the algorithm, y_{cut}. We define y_{23} as that value of y_{cut} at which the number of jets changes from two to three. The event sample is then split into subsamples having (approximately) the same number of events, according to the value of y_{23}, as shown in Table I. The three-jet configuration is chosen for each event and the jets are numbered

TABLE I

Subsamples defined by an interval of y_{23}, and the fraction of the sample for which jet 3 is the gluon jet.

JADE, y_{23}^J	jet 3 = g-jet	Durham, y_{23}^D	jet 3 = g-jet
0.000–0.009	90%	0.000–0.002	89%
0.009–0.023	85%	0.002–0.006	84%
0.023–0.056	81%	0.006–0.018	74%
0.056–1.000	69%	0.018–1.000	64%

according to decreasing jet energy, *i.e.*, jet 1 is the most energetic jet and jet 3 the least energetic. Small y_{23} corresponds to narrow two-jet events, large y_{23} to events with three or more well-separated jets.

The thrust axis is chosen as the z-axis with its positive direction such that the rapidity, $y_{\rm E}$, of jet 1 is positive, and the major axis is chosen as the y-axis with its positive direction such that jet 3 is in the positive major hemisphere. The rapidity distributions of particles assigned to each jet are shown in Fig. 1 for the four $y_{23}^{\rm D}$ intervals. We see that particles with $y_{\rm E} > 1$ come predominantly from a quark jet; with $y_{\rm E} < 1$ mostly from a quark jet; and with $-1 < y_{\rm E} < 1$ largely from the gluon jet.

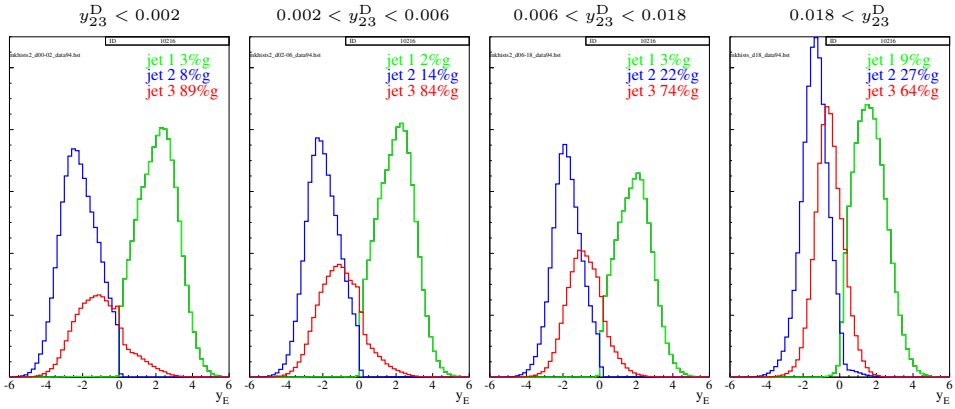

Fig. 1. Rapidity, $y_{\rm E}$, distributions of particles from jets 1, 2, and 3 for various $y_{23}^{\rm D}$ subsamples.

2. Results in one dimension, $R_2(Q)$

Fits of Eq. (1) are performed for each subsample, as well as for the entire sample. The estimates of α and R are very highly correlated. Therefore, to stabilize the fits, we fix the value of α to 0.443, the value found in a fit of the entire sample. Fits are also performed requiring the rapidity of the pair to be in a restricted region.

The resulting values of the effective radius, R, are shown in Fig. 2. It is seen that R increases as $y_{23}^{\rm D}$ is increased when no $y_{\rm E}$ selection is made or when $y_{\rm E} < -1$. For $-1 < y_{\rm E} < 1$, R is larger than for the other $y_{\rm E}$ regions, particularly at low $y_{23}^{\rm D}$. However, for $y_{\rm E} > 1$ and $y_{\rm E} < -2$, R is roughly independent of $y_{23}^{\rm D}$. It thus seems that the increase of R is associated with increasing importance of the gluon jet. Using $y_{23}^{\rm J}$ rather than $y_{23}^{\rm D}$ gives similar behavior.

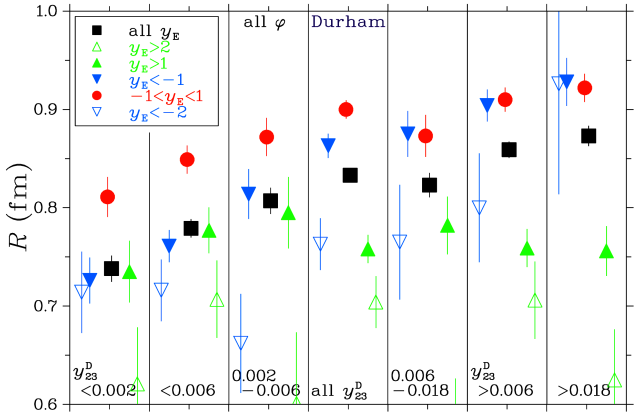

Fig. 2. Values of the effective radius, R, from fits of Eq. (1) for various y_{23}^{D} subsamples with selections on the rapidity, y_{E}, of the pair.

In addition to selecting intervals in y_{E}, we next select also intervals of the azimuthal angle of a track with respect to the y-axis (major axis), which is a measure of how close the track is to lying in the event plane. The resulting values of the effective radius, R, are shown in Fig. 3. For the two-jet region (small y_{23}) there is no significant dependence of R on the azimuthal angle. However, for the three-jet region R appears larger when the azimuthal angle is small, *i.e.*, when the particles lie in or near the event plane.

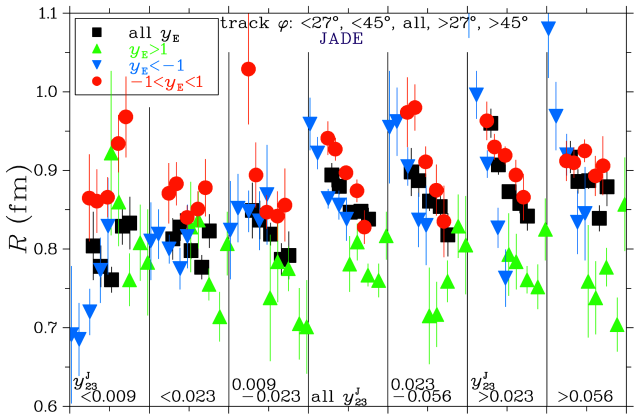

Fig. 3. Values of the effective radius, R, from fits of Eq. (1) for various y_{23}^{D} subsamples with selections on the rapidity, y_{E}, of the pair and on the azimuthal angle of the track with respect to the major axis.

3. Results in three dimensions, $R_2(\vec{Q})$

We now turn to a study of BEC in the Longitudinal Center of Mass System (LCMS) of the pair. The LCMS frame is defined as the frame, obtained by a Lorentz boost along the event (thrust) axis, where the sum of the three-momenta of the two pions $(\vec{p}_1 + \vec{p}_2)$ is perpendicular to the event axis. Assuming azimuthal symmetry about the event axis suggests that the region of homogeneity have an ellipsoidal shape with the longitudinal axis along the event axis.

In the LCMS frame, the event axis is referred to as the longitudinal direction, the direction of $\vec{p}_1 + \vec{p}_2$ as the out direction, and the direction perpendicular to these as the side direction. The components of $|\vec{p}_1 - \vec{p}_2|$ along these directions are denoted Q_{L}, Q_{out}, and Q_{side}, respectively. Since

$$\begin{aligned} Q^2 &= Q_{\mathrm{L}}^2 + Q_{\mathrm{side}}^2 + Q_{\mathrm{out}}^2 - (\Delta E)^2 && (3) \\ &= Q_{\mathrm{L}}^2 + Q_{\mathrm{side}}^2 + Q_{\mathrm{out}}^2 \left(1 - \beta^2\right) , \qquad \text{where} \quad \beta = \frac{p_{1\mathrm{out}} + p_{2\mathrm{out}}}{E_1 + E_2} , && (4) \end{aligned}$$

we replace R^2Q^2 in Eqs. (1) and (2) by

$$R^2Q^2 \Longrightarrow A^2 = R_{\mathrm{L}}^2 Q_{\mathrm{L}}^2 + R_{\mathrm{side}}^2 Q_{\mathrm{side}}^2 + \rho_{\mathrm{out}}^2 Q_{\mathrm{out}}^2 . \tag{5}$$

R_{L} and R_{side} are measures of the longitudinal and transverse size of the source, respectively, while ρ_{out} reflects both transverse and temporal sizes[1].

We incorporate Eq. (5) in Eqs. (1) and (2)

$$\begin{aligned} R_2(Q) &= \gamma \left[1 + \lambda \cos\left(\tan\left(\frac{\alpha\pi}{2}\right) A^{2\alpha}\right) \exp\left(-A^{2\alpha}\right)\right] \\ &\quad \times \left(1 + \epsilon_{\mathrm{L}} Q_{\mathrm{L}} + \epsilon_{\mathrm{side}} Q_{\mathrm{side}} + \epsilon_{\mathrm{out}} Q_{\mathrm{out}}\right) . \end{aligned} \tag{6}$$

We also investigate the decomposition

$$\begin{aligned} Q^2 &= Q_{\mathrm{L}}^2 + Q_{\mathrm{side}}^2 + q_{\mathrm{out}}^2 , \qquad q_{\mathrm{out}}^2 = Q_{\mathrm{out}}^2 - (\Delta E)^2 , \\ A^2 &= R_{\mathrm{L}}^2 Q_{\mathrm{L}}^2 + R_{\mathrm{side}}^2 Q_{\mathrm{side}}^2 + r_{\mathrm{out}}^2 q_{\mathrm{out}}^2 , \end{aligned} \tag{7}$$

which corresponds to the LCMS frame boosted to the rest frame of the pair. Its three components are invariant under Lorentz boosts along the out direction. Note that r_{out} is a proper radius; unlike ρ_{out} there is no dependence on ΔE.

[1] In the literature, the coefficient of Q_{out}^2 in Eq. (5) is usually denoted R_{out}^2. We prefer to use ρ_{out}^2 to emphasize that, unlike R_{L} and R_{side}, ρ_{out} contains a dependence on β.

Fits in both frames should, in principle, yield the same values of R_{L} and R_{side}. However, there is a systematic shift (about 0.8 fm for R_{L}). For both frames, the results are consistent with no dependence of R_{L}, ρ_{out} and r_{out} on y_{23}, while R_{side} increases with y_{23}. The systematic shift cancels in the ratio, and we, therefore, plot the ratio in Fig. 4. We see that R_{side} increases with y_{23}^{J}; the increase is less for $y_{\mathrm{E}} > 1$ than for the other y_{E} intervals. However, no significant dependence on y_{23} is observed in any of the y_{E} intervals for R_{L}, ρ_{out}, or r_{out}.

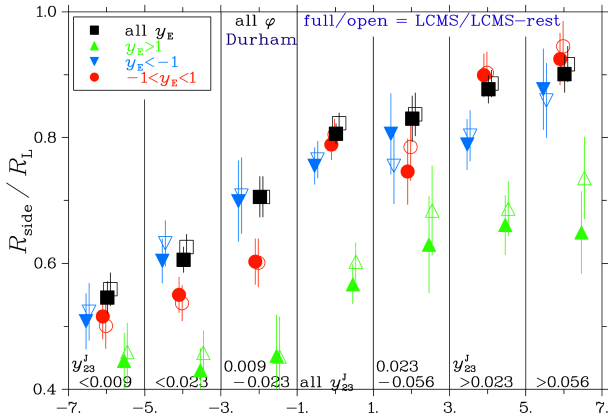

Fig. 4. Values of the ratio of the radii, $R_{\mathrm{side}}/R_{\mathrm{L}}$, from fits of Eq. (6) with Eqs. (5) and (7) for various y_{23} subsamples with selections on the rapidity, y_{E}, of the pair.

It is interesting to examine the ratio of R_{side} to r_{out}. Since r_{out} is approximately constant and R_{side} increases with y_{23}, this ratio also increases. The value is about 0.4 for the lowest y_{23} and about 0.7 at the highest y_{23}. Thus the shape is not azimuthally symmetric about the event axis, not even for narrow two-jet events. In fact, it is the least symmetric for the narrowest two-jet events. The ratio r_{out} to R_{L} is about 1.2–1.3.

Further, we find that the out direction tends to lie in the event plane. This is shown in Fig. 5, where we see the azimuthal angle of the out direction with respect to the major direction to be strongly peaked at zero for well-separated three-jet events ($0.056 < y_{23}^{\mathrm{J}}$) when $y_{\mathrm{E}} < -1$ or $-1 < y_{\mathrm{E}} < 1$. It is much less peaked for $y_{\mathrm{E}} > 1$ and for all y_{E} intervals of narrow two-jet events.

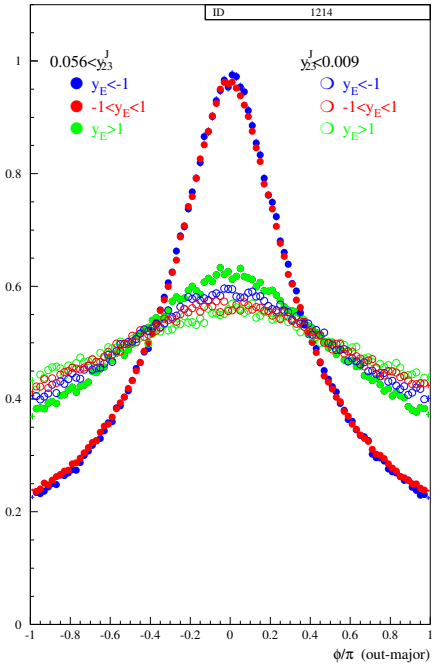

Fig. 5. The azimuthal angle of the out direction with respect to the major direction for well-separated three-jet events and for narrow two-jet events for three intervals of pair rapidity, y_{E}.

4. Conclusion

From the one-dimensional fits, we found that R increases with y_{23}, but not in "pure quark" regions ($y_{\mathrm{E}} > 1$ or $y_{\mathrm{E}} < -2$ and, for narrow two-jet events, $y_{\mathrm{E}} < -1$). This suggests that the increase in R is due to the gluon jet. Further, for three-jet events R is larger for particles in the event plane.

The three-dimensional analysis showed that the increase in R is predominantly due to an increase in R_{side}, the other components of R showing little or no dependence on y_{23}.

The picture we get of the region of homogeneity is a squashed ellipsoid slightly shorter (longitudinal axis) than it is wide (in the out direction) and thin (in the side direction). The longitudinal and out dimensions are rather independent of y_{23}. However, the side dimension increases as one goes from narrow two-jet events to well-separated three-jet events. At the same time, in the rapidity regions, where the gluon plays a role ($y_{\mathrm{E}} < 1$), the out direction lies preferentially in the event plane. In "pure quark" jets (narrow two-jet events or three-jet events with $y_{\mathrm{E}} > 1$), the ellipsoid is approximately isotropically oriented about the thrust axis. In other cases, the out axis tends to lie in the event plane.

REFERENCES

[1] P. Achard *et al.* [L3 Collaboration], *Eur. Phys. J.* **C71**, 1648 (2011).
[2] T. Csörgő, J. Zimányi, *Nucl. Phys.* **A517**, 588 (1990).
[3] T. Csörgő, W. Kittel, W.J. Metzger, T. Novák, *Phys. Lett.* **B663**, 214 (2008).